MATERIAL IDENTIFICATION FOR THE DESIGN OF COMPOSITE ROTARY WINGS

ICAS-82-2.4.4

V.Giavotto, C.Caprile, M.De Capitani, L.Salvioni
Aerospace Department, Politecnico Milano, Italy
and
V.Caramaschi, G.C.Maffioli, F.Mussi
C.A.G.AGUSTA S.p.A., Cascina Costa, Italy

Abstract

Among the developments that appear to be absolutely needed for the design of advanced composite rotary wings there are material models, to be supported by substantial experimentation and to be capable of an accurate modeling of the behaviour of multilayer FRPs, complete of failure criteria regarding all possible failure modes. This paper reports an experimental activity carried on by Aerospace Department of Politecnico of Milano in cooperation with Costruzioni Aeronautiche G.Augusta. The most relevant part of such activity has been a fairly large campaign on tubolar specimens in biaxial stress states and plane specimens in uniaxial stress states. All tests have been run statically, measuring stresses and strains up to failure. The results of such measurements have been so far worked out to verify existing material models and failure criteria. No one existing failure criteria seems to be completely adeguate to the whole stress domain explored.

1. Foreword

The use of composite materials in the design of rotary wing components is quite widespread nowadays [1]-[3]. Such materials, which are generally made of high performance fibers with a smaller quantity of epoxy resin, may give appreciable advantages on conventional metal designs, provided the designer can rely on accurate material data and design procedures. In this field Agusta has developed, for the helicopter A109B, a composite main rotor (fig.1), which has almost completed ground testing, and which will be flown in the near future.

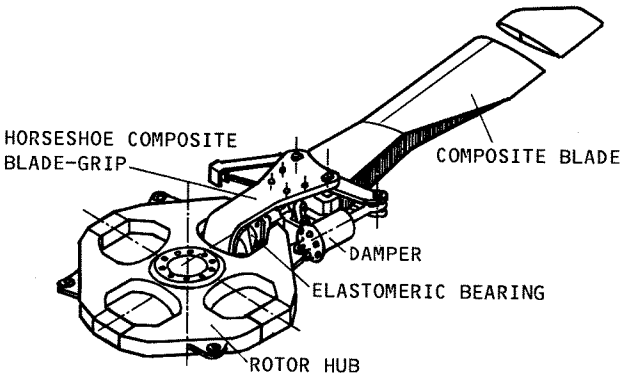

FIGURE 1 - A 109B MAIN ROTOR ASSEMBLY

For the development of such a rotor much research work has been carried on, mostly in cooperation with the Aerospace Department of Politecnico di Milano, under the contracts no. 432, 781, 782.

The objectives, the plan and some of the results of this research activity has been already presented in previous papers [1],[4].

The present paper reports some results of an experimental activity, not yet concluded, aimed to check, and possibly improve, material models to be used in the design process.

As for the usual metallic materials, what designers need from material models is the possibility of predicting, with good or at least known accuracy:

- elastic behaviour;
- elastic limits, and possibly behaviour beyond elastic limits;
- failure.

For some design, material models should be suited also for threedimensional states of stress.

2. Introduction

In the elastic range composites are usually modeled as linear anisotropic materials [5], whose moduli are obtained from a limited number of specimens with uni-directional fibers, in simple stress states. Figures 2 and 3 show the results of typical simple stress tests, with best-fit polynomial approximations used to evaluate moduli at zero stress.

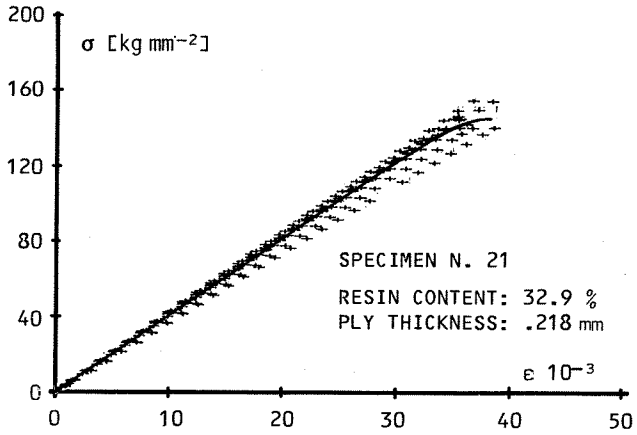

FIGURE 2 - POLYNOMIAL BEST FIT; σ-ε CURVE

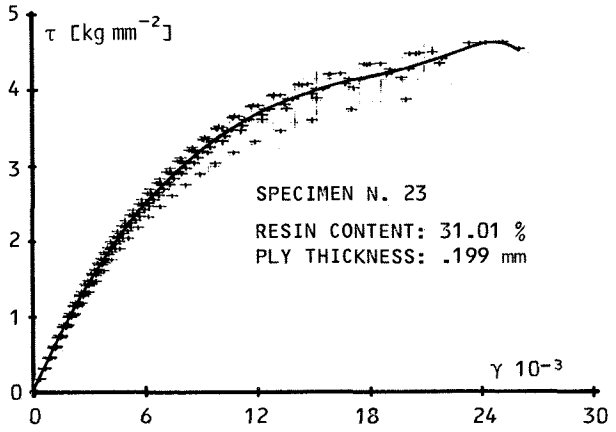

FIGURE 3 - POLYNOMIAL BEST FIT; τ-γ CURVE

By combining the properties of the different unidirectional layers present in the composite, anisotropic moduli are easily obtained, identifying a linear material model, which can be quite accurate as long as the composite behaviour remains linear. Usually, since the fibers alone tend to show a linear behaviour up to very high stresses, a linear model for the complete composite can be adeguate as long as the stresses in the resin remain low; this often happens to a well designed structural element in the normal load conditions, because obviously in these cases the fibers must carry the most of the stresses.

So elastic material models can be very useful to evaluate stiffnesses and dynamic properties, but they cannot be easily used to evaluate the boundary of the elastic range.

One outstanding feature of such linear anisotropic models is that the moduli of a composite (or a laminate) made of different unidirectional layers (or laminae) can be obtained with good accuracy by proper combination of the moduli of the laminae.

In other words, knowing a limited number of parameters (for uni-directional laminae) the designer can optimize a laminate, for given stress conditions and/or given stiffnes requirements.

For the prediction of elastic boundaries and of material behaviour slightly beyond such boundaries very little is known from the literature. A simple model has been developed, to be used with existing non-linear F.E. programs, consisting on the superimposition of two different materials (say material A and material B), each filling all the volume, being:

A - an anisotropic elastic material incorporating the moduli of fibers alone;

B - an isotropic elastic-plastic material, obeying von Mises' strain hardening law.

The properties of material B are so chosen that the superimposition of the two materials gives the best possible approximation of laminate behaviour. Although rather elementary, such a model offers some basic advantages which make it interesting, at least for the preliminary stages.

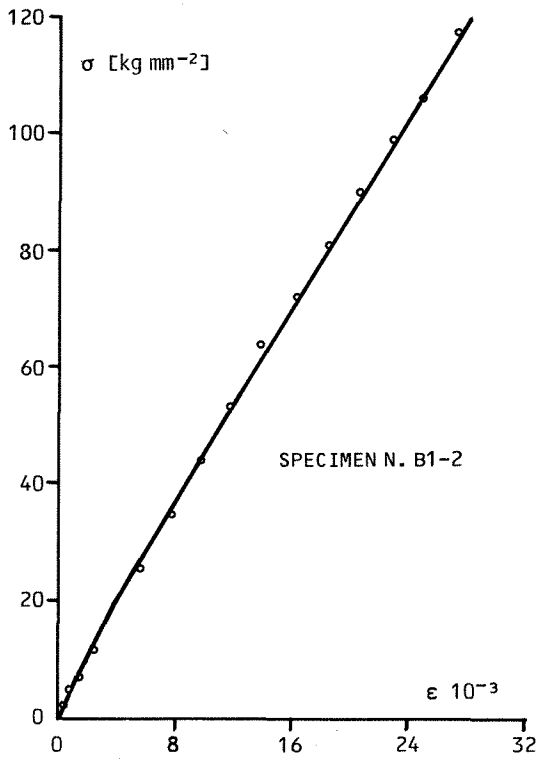

FIGURE 4 - TWO PHASE MATERIAL MODEL
COMPARISON OF F.E. WITH EXPER. DATA

Figures 4 and 5 show comparison of experimental data from simple stress tests on two laminates differing only in lamina layups, and the corresponding non linear F.E. analysis, made by the program ADINA with the model outlined above.

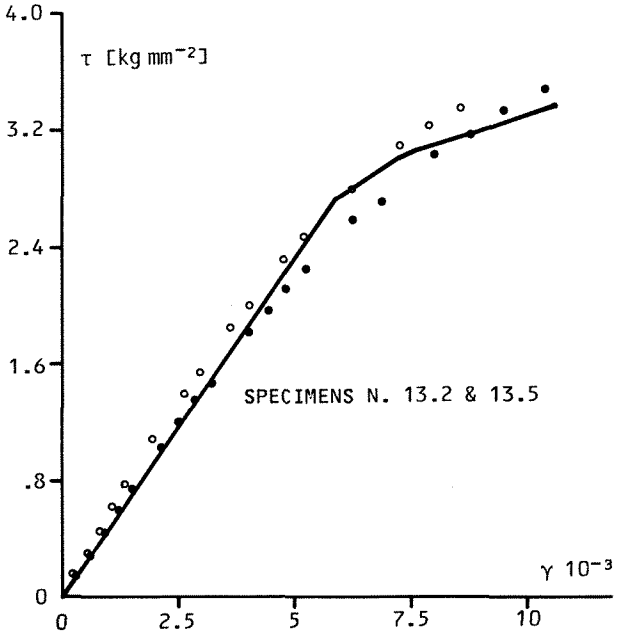

FIGURE 5 - TWO PHASE MATERIAL MODEL
COMPARISON OF F.E. WITH EXPER. DATA

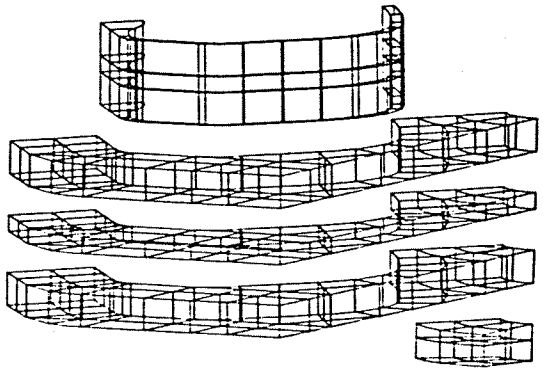

FIGURE 6 - 3D F.E. MESH OF 1/8 HUB

Figure 6 shows the F.E. mesh of 1/8 of the rotor hub in Figure 1 (quadratic isoparametric elements) which was used for improving the first design and to predict the behaviour beyond elastic limits.

The comparison of F.E. analyses with static tests on the complete article was satisfactory, up to the first local failures, which occurred definitely beyond elastic limits.

A large literature is available on failure criteria for laminates in plane stress, but here the state of the art is not completely satisfactory.

The proposed failure criteria have been extensively checked by comparison withe experimental data [10]-[12]; no one of them seems to be able to cope with all actual failures, with the exception of the Puppo-Evensen Criterion, which was found to be adequate for predicting the failure of certain types of laminates [10].

The proposed failure criteria can be grouped in two large categories, i.e. lamina failure criteria and laminate failure criteria [13].

Lamina failure criteria are usually based on lamina stresses, computed with some linear model from the average laminate stresses.

Their major limitations come from the fact that lamina stresses at failure generally do not conform to a linear laminate model, and that the failure of a single lamina may not correspond to the failure of the whole laminate.

So lamina failure criteria, as it has been already pointed out [11], tend to be exceedingly conservative.

On the other hand, laminate failure criteria [6]-[9] identify a failure envelope, which is a convex surface in the stress space enclosing all the points where the laminate does not fail.

It is quite obvious that any such surface can always be adequately approximated by one or more stress polynomials, provided the degree and/or the number of such polynomials, i.e. the number of parameters to be measured is high enough.

As it has been pointed out by Wu [8], the number of such parameters can be considerably large, thus requiring a large number of tests to identify the failure locus of each particular laminate. But the main advantage of laminate failure criteria on lamina failure criteria is that the former can intrinsically account for lamina interactions. In any case a good failure criterion should also provide the designer the mean for predicting the ultimate strength of laminates obtained by combining a certain number of elementary laminae with different fiber orientations, without requiring special strength tests for each selected stacking layup.

Actually the usual linear anisotropic material models and the elastic-plastic model outlined above have this property, as their parameters can be obtained by proper combination of the component laminae, without requiring special tests for each designed layup.

So it seems to be useful ro search for failure criteria requiring only some kind of lamina strength data, but without the intrinsic limitation of lamina failure criteria, then incorporating some interaction model.

The search of such a failure criterion was one of the objectives of the research work reported in this paper.

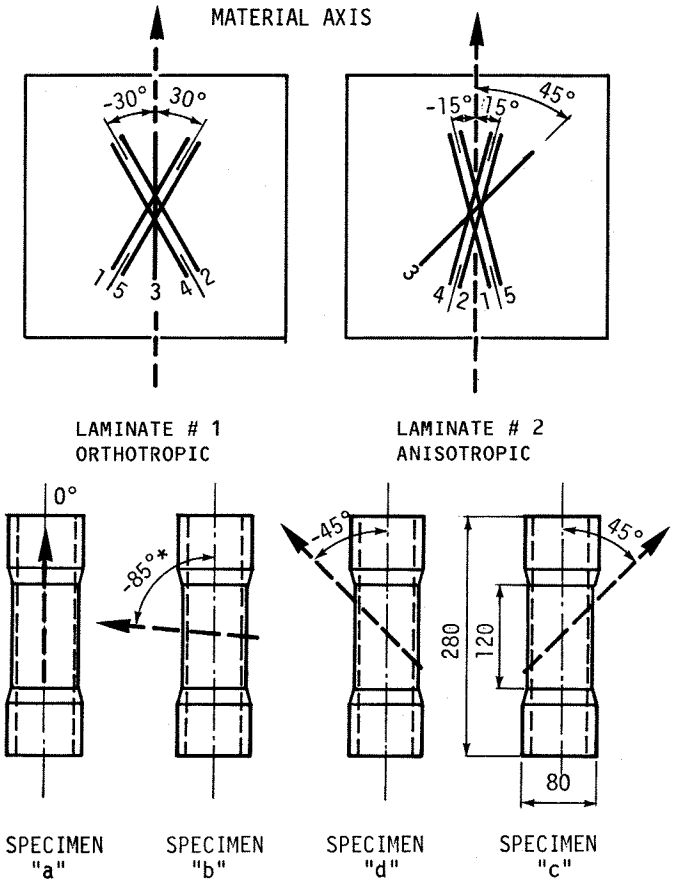

* 85° INSTEAD OF 90° TO AVOID OVERLAPPING JOINT

FIGURE 7 - LAMINATE LAYOUT & TUBULAR SPECIMENS

3. The Experimental Plan

The experimental plan includes testing of tubular specimens under combined loads and of flat specimens under pure axial load.

In the first part of the investigation tubular specimens were loaded in axial tension and torsion, while in a subsequent part they will be also subject to internal pressure.

Two glass fiber/epoxy laminates have been selected for the experiments, where the layers are arranged as indacated in figure 7, with a thickness of 2.4 mm for tubular specimens and 1.2 for flat specimens.

Tubular specimens are made in such a way that the laminate reference direction x is at 0°, 90°, +45° and -45° to the axis of the specimen (specimens "a" "b","c", and "d" in Figure 7).

This way an appreciable range of stress combinations can be achieved.

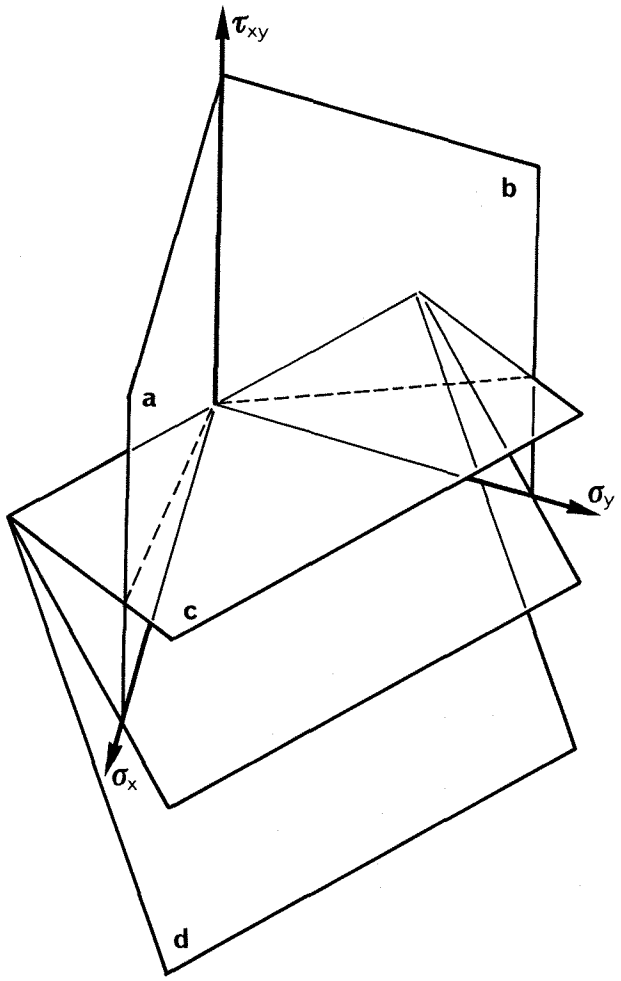

FIGURE 8 - STRESS LOCI FOR THE DIFFERENT SPECIMENS

In fact, if x and y are the laminate reference axes, it is apparent that, in the stress space, the stress combinations of specimens "a" and "b" lay, respectively, on $\sigma_x - \tau_{xy}$ and $\sigma_y - \tau_{xy}$ plane, and the ones of specimens "c" and "d" lay on the planes $2\tau_{xy} = \pm(\sigma_x + \sigma_y)$ (Figure 8)

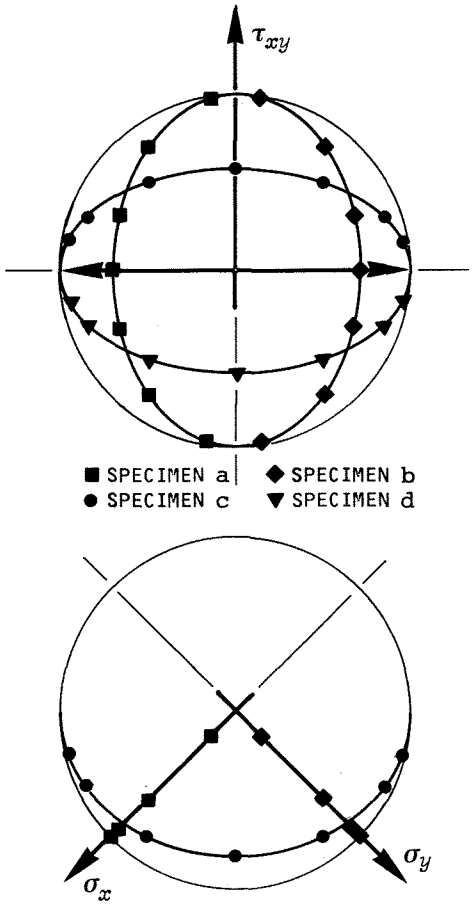

FIGURE 9. - STRESS CONDITIONS OF TUBULAR SPECIMENS

Through seven values selected for the torsional to axial stress ratio, 28 laminate stress combinations can be obtained in the 4 specimen types; such combinations, shown in Figure 9, appear to be fairly well distributed in the half space where tensile stress prevails ($\sigma_x + \sigma_y > 0$)

For the first laminate only one of the two specimen types "c" or "d" is needed, due to laminate orthotropy.

Then a total of 258 tubular specimens has been planned.

Figure 10 shows the ensemble of the testing equipment, whose loading and measuring schemes are reported, respectively, in Figures 11 and 12. Figure 13 is a detail view of the equipment, including specimen.

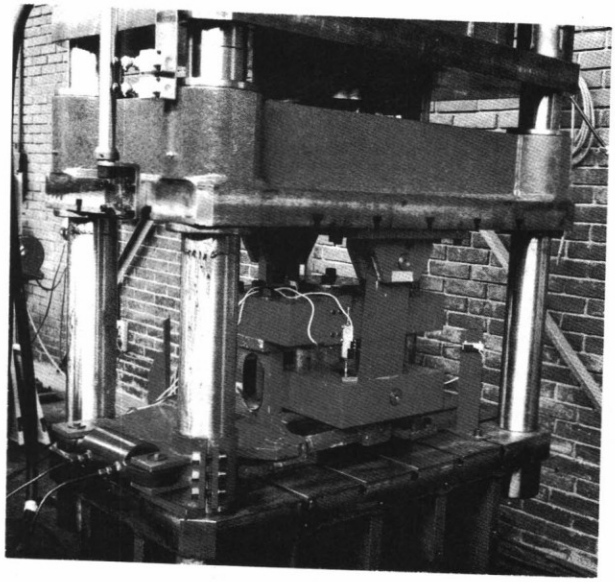

FIGURE 10 - TUBULAR SPECIMEN TEST EQUIPMENT

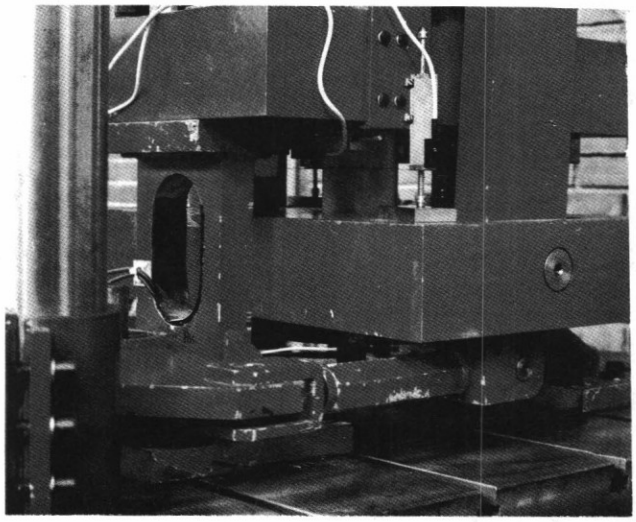

FIGURE 13 - DETAIL OF THE TEST APPARATUS

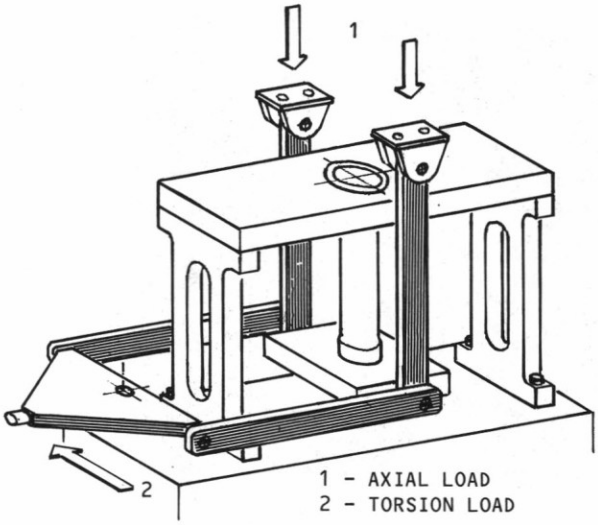

FIGURE 11 - LOADING SYSTEM (SCHEMATIC)

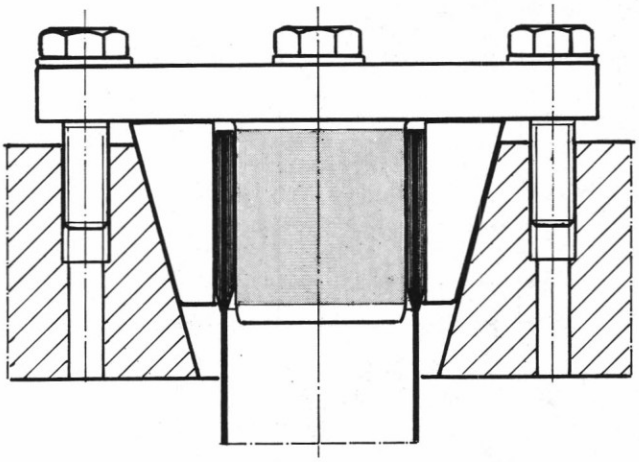

FIGURE 14 - TUBULAR SPECIMEN GRIP SYSTEM

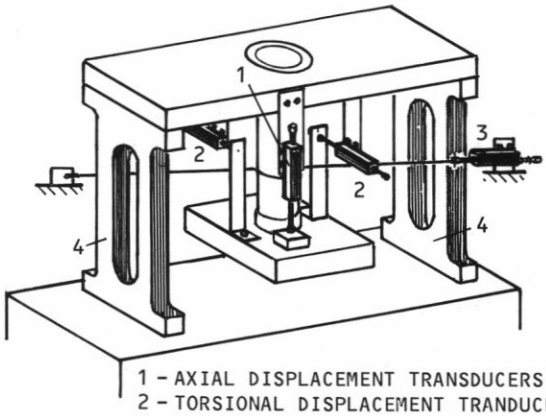

FIGURE 12 - MEASUREMENT SYSTEM

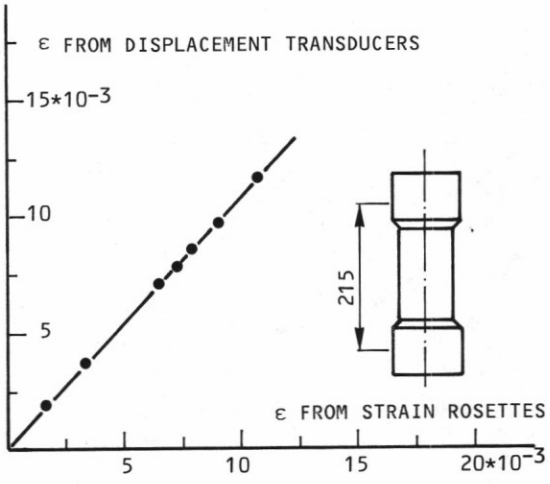

FIGURE 15 - AXIAL STRAIN CALIBRATION

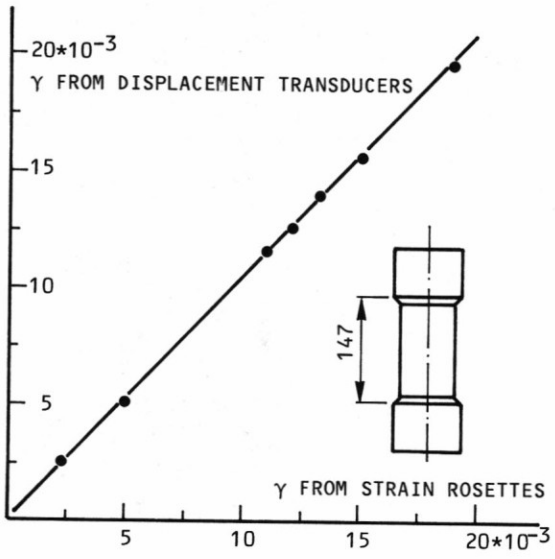

FIGURE 16 - TORSIONAL STRAIN CALIBRATION

End grips, shown in Figure 14, proved to work properly in every load condition tested.

For calibration purposes three specimens were equipped with strain gage rosettes; the strains recorded from strain gages and the ones obtained from displacement transducers are in excellent agreement (Figures 15 and 16), provided the effective tube length displayed in Figures 15 and 16 are used to compute strains from displacements.

Flat tensile specimens are also made with laminate axis at angles of 0°, 90°, 45° and -45° to specimen axis. The load combination of such specimens are represented in the stress space by the points in Figure 17.

The purpose of such specimens is to check the correlations between flat and tubular specimen tests, and to study the effect of specimen width. For this reason a total of 168 flat specimens are included in the plan having 25.4, 38.1, 50.8 and 63.5 mm widths.

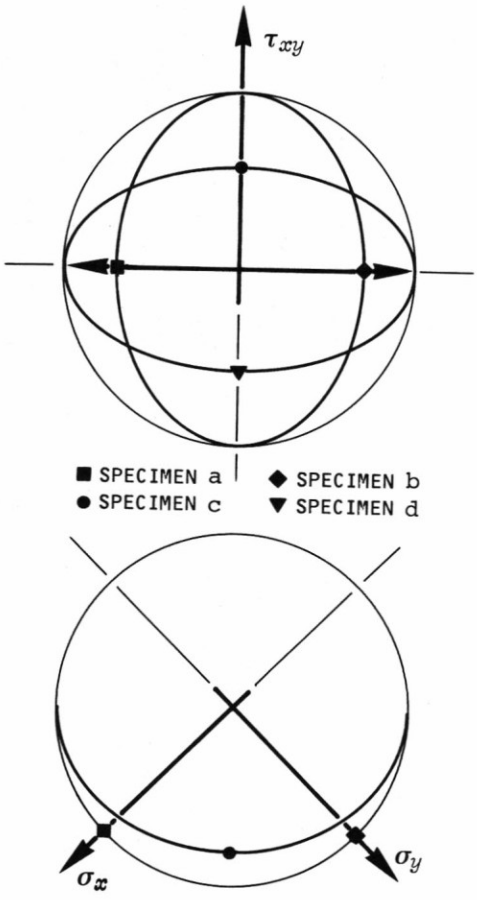

FIGURE 17 - STRESS CONDITIONS OF FLAT SPECIMENS

FIGURE 18 - SWINGING GRIPS FOR FLAT SPECIMENS

Swinging grips have been developed (Figure 18) allowing for the shear strains that may arise in a tensile test, when orthotropy axes are not aligned to specimen axis.

4. Test Results

About one third of the tubular specimens and one half of the flat specimens have been tested so far. Figure 19 shows a part of the broken tubular specimens.

FIGURE 19 - SOME OF THE SPECIMENS TESTED

Five different failure modes were observed, having the following dominant factors:

1 - Fiber tensile failure (Figure 20) O

2 - Inter-fiber failure of internal layers (Figure 21) Δ

3 - Inter-fiber failure of external layers □

4 - Fiber compressive failure (fiber instability) ▽

5 - Global instability (Figure 22) ✻

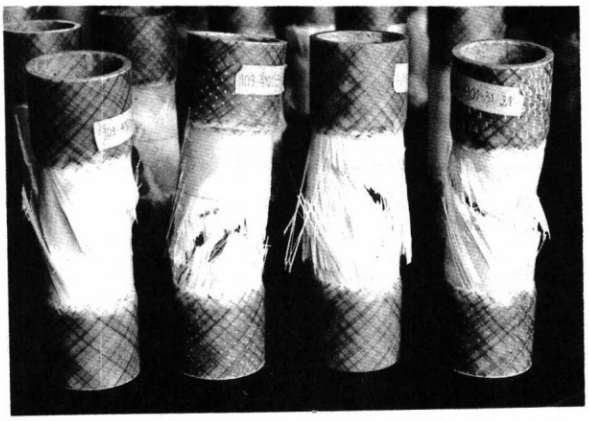

FIGURE 20 - TYPICAL FAILURES (MODE 1)

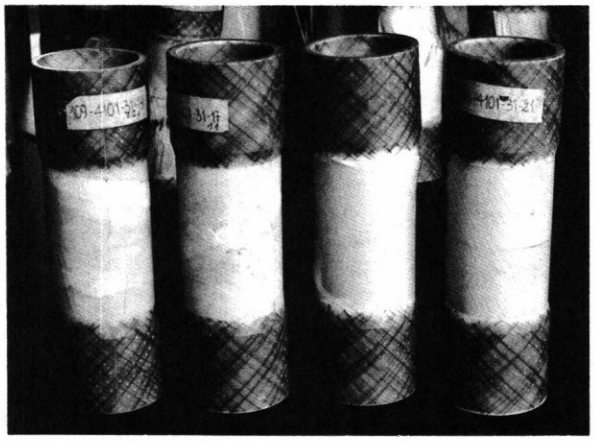

FIGURE 21 - TYPICAL FAILURES (MODE 2)

For flat tensile specimens of all widths the first 3 failure modes were also observed (Figures 23-25); obviously the last two, requiring sensible compression, could not occur in this specimens. Figure 26, corresponding to failure mode 2, shows a remarkable shear deformation that was allowed by the end grips.

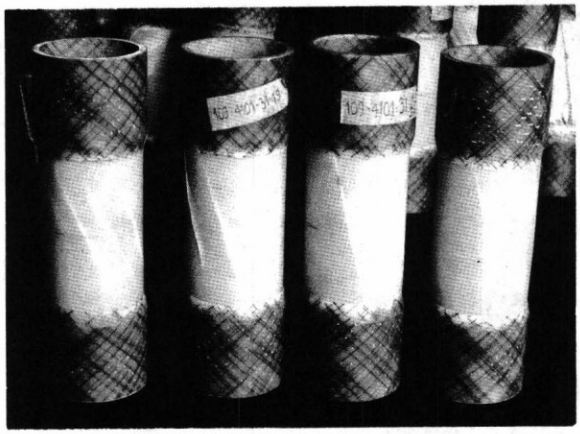

FIGURE 22 - TYPICAL FAILURES (MODE 5)

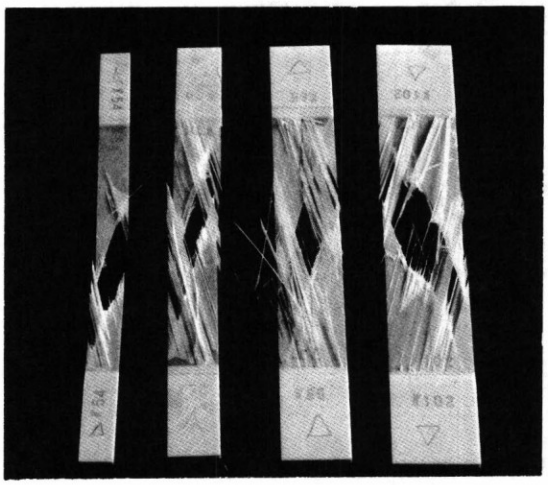

FIGURE 23 - TYPICAL FAILURES (MODE 1)

FIGURE 24 - TYPICAL FAILURES (MODE 2)

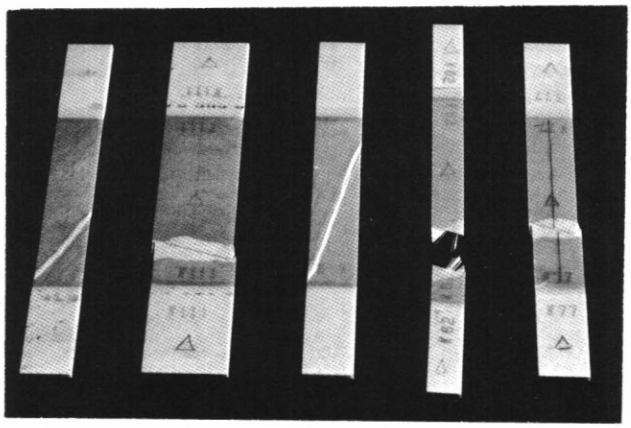

FIGURE 25 - TYPICAL FAILURES (MODE 3)

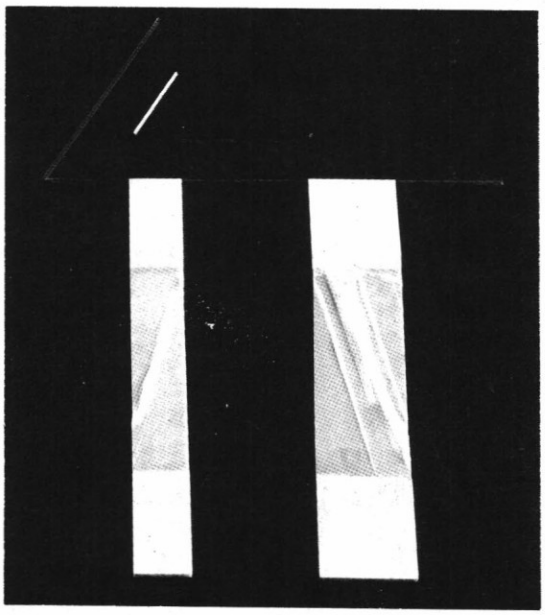

FIGURE 26 - SHEAR STRAIN ALLOWED BY GRIPS

Figures 27 to 33 report all the failure stresses of the tubular specimens with a different symbol for each failure mode, together with the average failure stresses of the corresponding flat specimens (the black filled symbols).

Such stress values are represented in the laminate $\sigma_x - \tau_{xy}$ plane for specimens "a", in $\sigma_y - \tau_{xy}$ plane for specimens "b", and in the projection of "c" and "d" planes on $\sigma_x - \sigma_y$ plane, for specimens "c" and "d". A good correlation seems to exist between flat specimen and tubular specimen failure stresses.

Figure 34 and 35 report the failure normal stresses (referred to specimen reference) for the two laminates. Such stresses do not show a clear correlation to specimen width.

During each test torsional, axial and circumferential deflection of tubular specimens were automatically recorded, together with the applied twisting moments and axial forces.

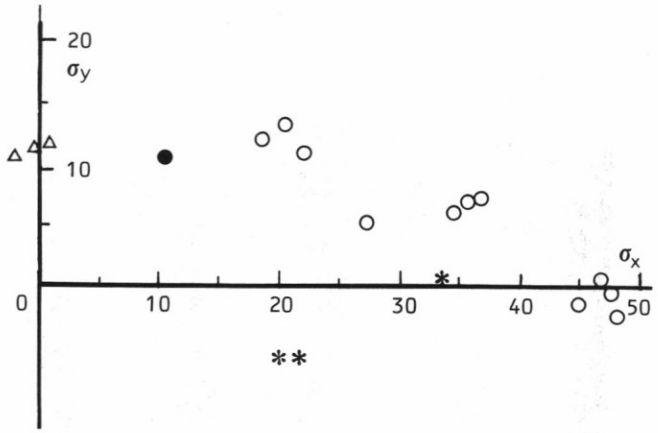

FIGURE 29 - ORTHOTROPIC LAMINATE FAILURE STRESSES OF SPECIMENS "c" [kgmm^{-2}]

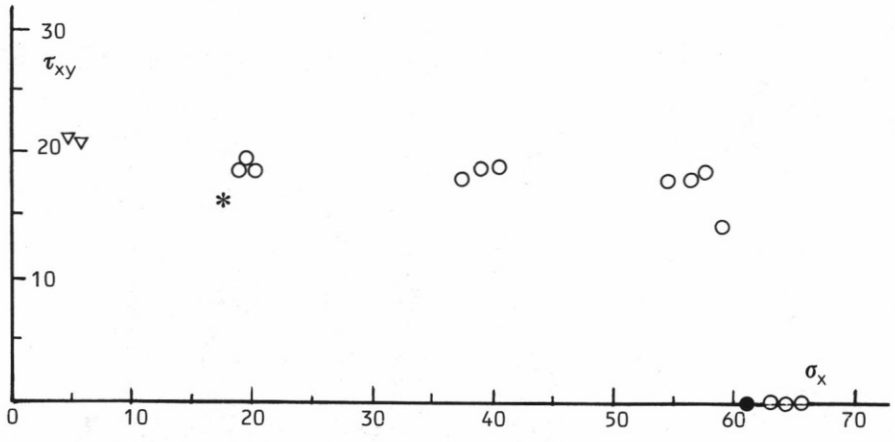

FIGURE 27 - ORTHOTROPIC LAMINATE FAILURE STRESSES OF SPECIMENS "a" [kgmm^{-2}]

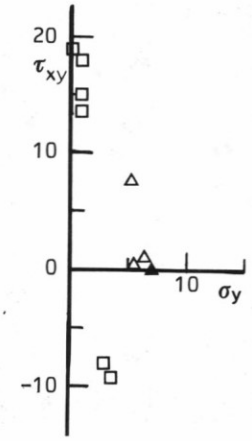

FIGURE 28 - ORTHOTROPIC LAMINATE FAILURE STRESSES OF SPECIMENS "b" [kgmm^{-2}]

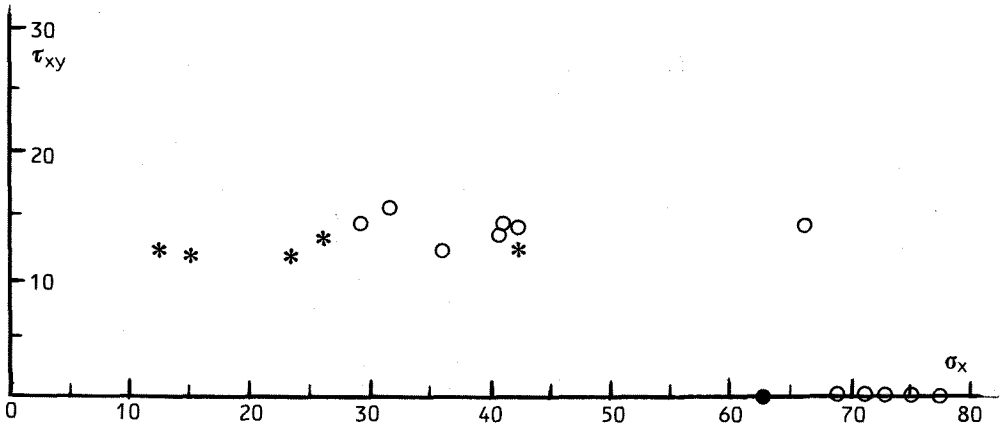

FIGURE 30 - ANISOTROPIC LAMINATE
FAILURE STRESSES OF
SPECIMENS "a" [kgmm^{-2}]

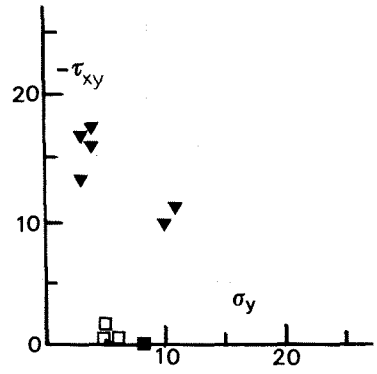

FIGURE 31 - ANISOTROPIC LAMINATE
FAILURE STRESSES OF
SPECIMENS "b" [kgmm^{-2}]

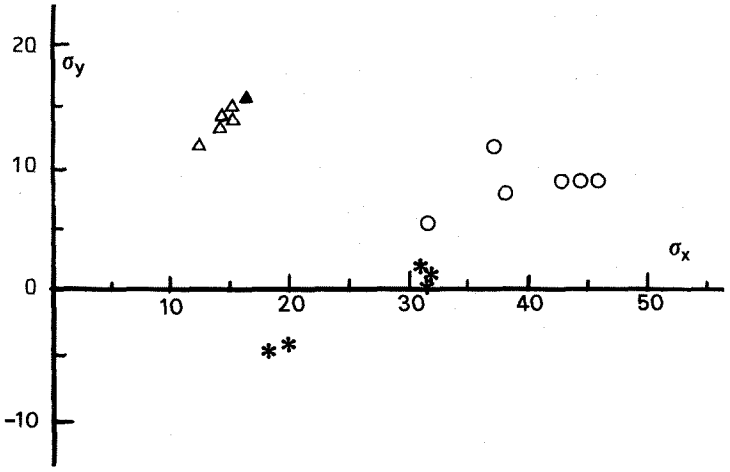

FIGURE 33 - ANISOTROPIC LAMINATE
FAILURE STRESSES OF
SPECIMENS "d" [kgmm^{-2}]

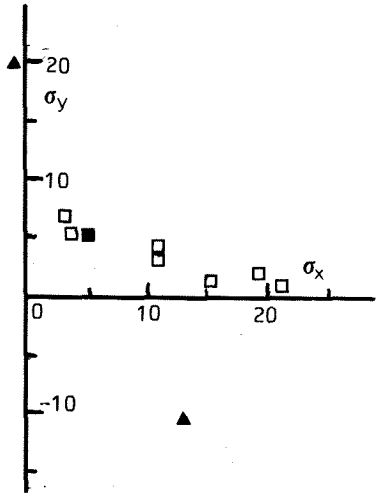

FIGURE 32 - ANISOTROPIC LAMINATE
FAILURE STRESSES OF
SPECIMENS "c" [kgmm^{-2}]

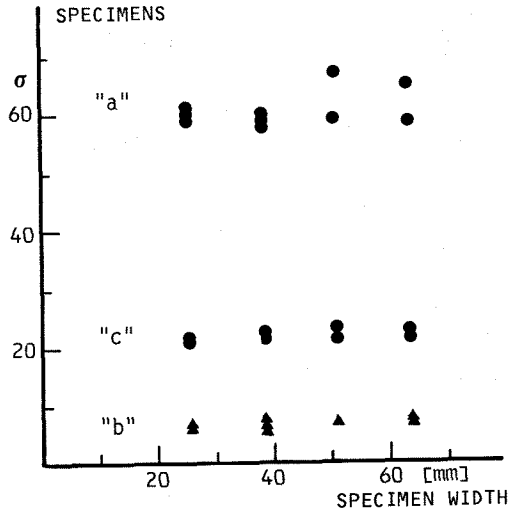

FIGURE 34 - ORTHOTROPIC LAMINATE
FAILURE STRESSES OF
FLAT SPECIMENS [kgmm^{-2}]

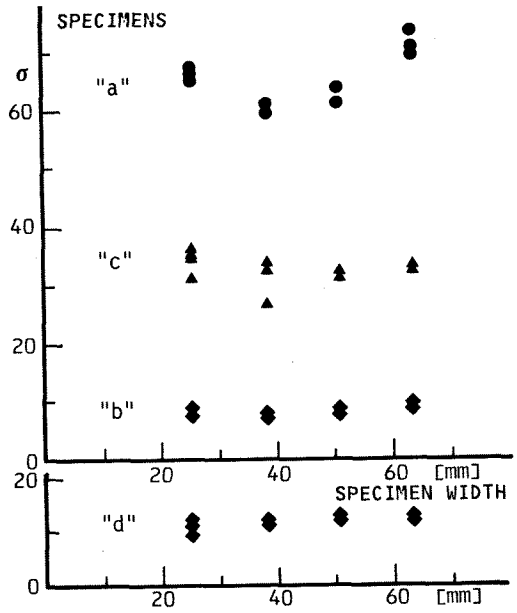

FIGURE 35 - ANISOTROPIC LAMINATE FAILURE STRESSES OF FLAT SPECIMENS [$kgmm^{-2}$]

5. Evaluation of Linear Material Models

To evaluate the accuracy of linear material models, linear analyses were firstly performed with the program HANBA2 (which requires a F.E. idealization only on specimen cross-section [14]) employing the material models identified in the usual way.

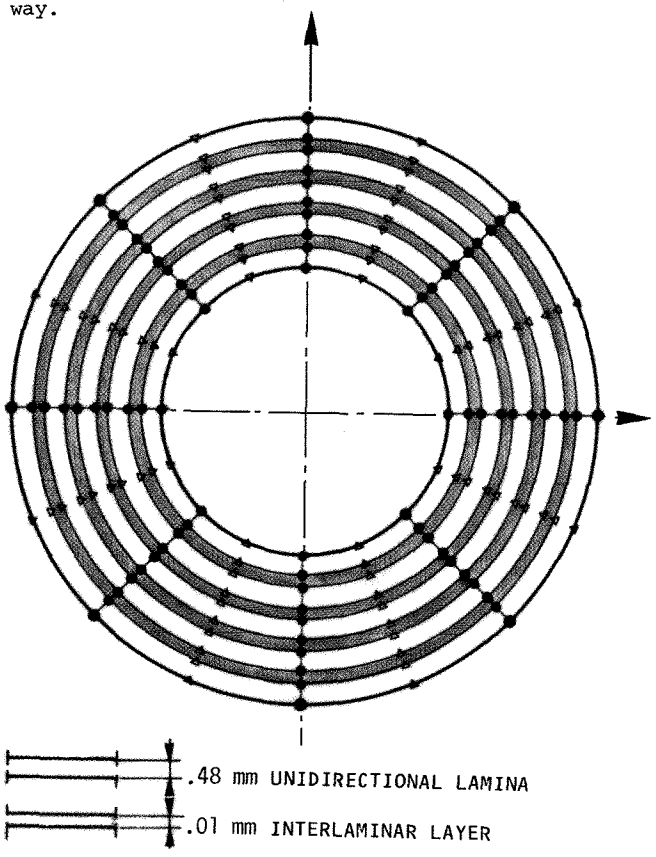

FIGURE 36 - IDEALIZATION OF TUBULAR SPECIMEN SECTION (THICKNESS NOT TO SCALE)

Figure 36 reports the idealization used; the analyses gave the section stiffness and compliance matrices, together with lamina and interlaminar stresses in unit load conditions.

Torsional and axial deflections corresponding to relatively low loads were then extracted from all the test recordings, and compared with the theoretical values, computed for the same loads by means of the section compliances from HANBAZ analyses.

Figures 37 and 38 report the distribution of the differences between theoretical and experimental deflections; as it was expected such differences are reasonably low, so strengthening the previous statement that the usual linear material models are generally satisfactory.

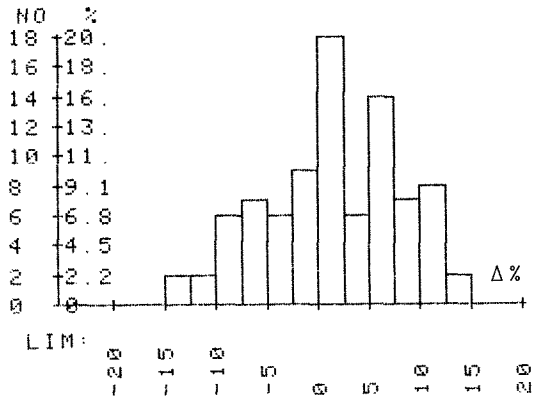

FIGURE 37 - DISTRIBUTION OF DIFFERENCES BETWEEN THEORETICAL & EXPER. AXIAL DISPLACEMENTS

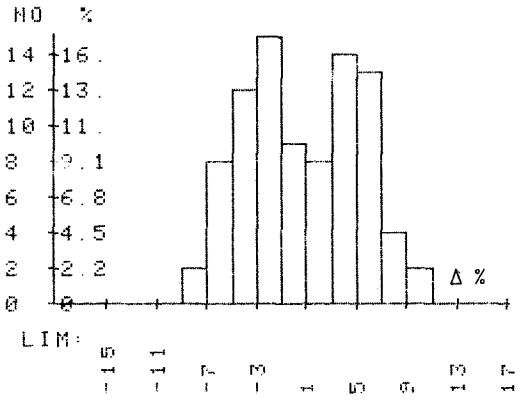

FIGURE 38 - DISTRIBUTION OF DIFFERENCES BETWEEN THEORETICAL & EXPER. TORSIONAL DISPLACEMENTS

6. Lamina Failure Criteria

The lamina stresses at failure were computed for tubular specimens, by combining the unit load stresses from linear analysis, multiplied by failure loads (axial force and twisting moment), i.e. assuming a stress distribution corresponding to linear material behaviour. With the same procedure interlaminar stresses at failure were also computed.

Figures 39, 40 and 41 report the distribution of the longitudinal normal stresses σ_L (along fiber direction), of the transverse normal stress σ_T and of the shear stress τ_{LT} of all laminae of tubular specimens at failure. From such distribution the following "reliable" maximum were estimated:

$$\sigma_{L,MAX} = 108 \text{ Kg mm}^{-2}$$

$$\sigma_{T,MAX} = 42 \text{ Kg mm}^{-2}$$

$$\tau_{LT,MAX} = 38 \text{ Kg mm}^{-2}$$

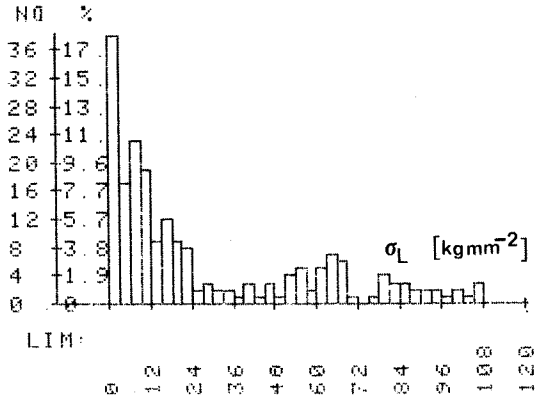

FIGURE 39 - DISTRIBUTION OF LAMINA STRESSES AT FAILURE

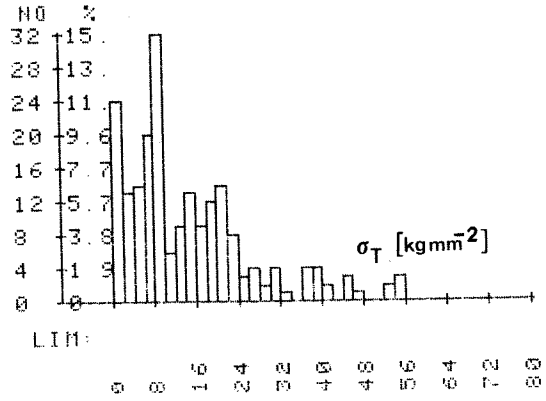

FIGURE 40 - DISTRIBUTION OF LAMINA STRESSES AT FAILURE

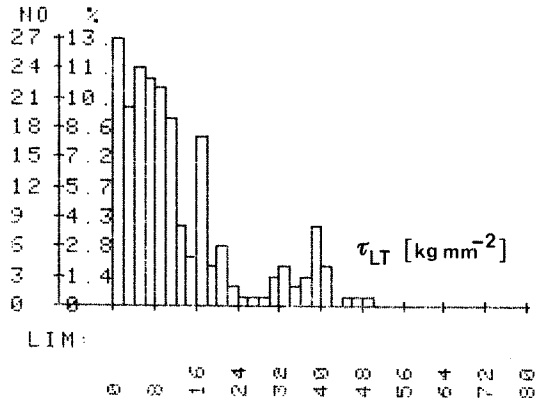

FIGURE 41 - DISTRIBUTION OF LAMINA STRESSES AT FAILURE

Such stresses were then assumed as equivalent lamina failure stresses for simple stress conditions, and they were used to evaluate different failure criteria. The best results seem to be the ones obtained with the Tsai-Hill criterion: figure 42 reports the distribution of the values of Tsai-Hill formula (the highest lamina value for each specimen).

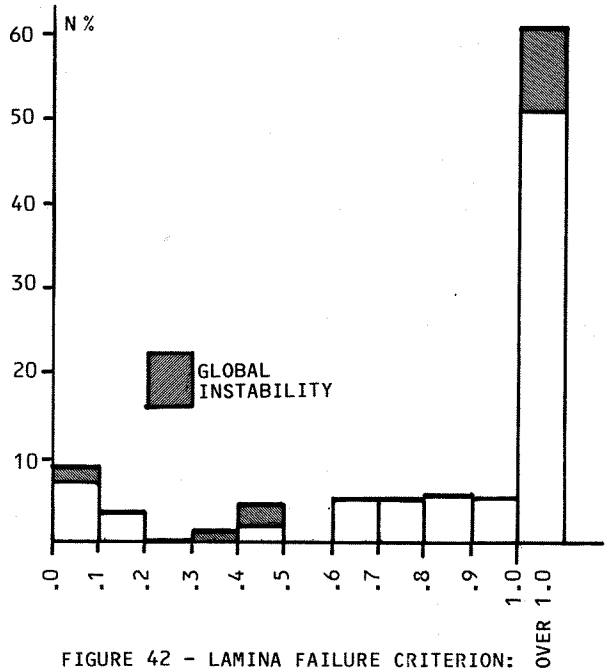

FIGURE 42 - LAMINA FAILURE CRITERION: DISTRIBUTION OF THE VALUE OF TSAI-HILL FORMULA

It may be noted that the strength of a large number of specimens is underestimated (a large number of values exceeds unity, with a maximum around 4), but for a non negligible number of specimen it is overestimated. This cannot be explained by interlaminar failure, as the interlaminar stresses computed as mentioned above, never exceeded .2 Kg mm^{-2}, nor by general instability, which occurred only in a limited number of cases.

7. Laminate Failure Criteria

For the orthotropic laminate the Puppo-Evensen (9) failure criterion has been checked; the corresponding failure boundaries are reported as ditted lines in figures 43-45: they do not follow very closely the experimental trends, so confirming Wu's statement (8) that phenomenological failure criteria may require a larger number of parameters.

A quite different failure criterion has then been developed as follows.

A rough elastic-plastic stress analysis was performed, assuming for each lamina the following non-interacting stress model:

$$\sigma_L = E_L \, \varepsilon_L$$

$$\sigma_T = \begin{cases} E_T \, \varepsilon_T & \text{for } \bar{\sigma}_{T-} \leq E_T \varepsilon_T \leq \bar{\sigma}_{T+} \\ \bar{\sigma}_{T-} & \text{for } E_T \varepsilon_T \leq \bar{\sigma}_{T-} \\ \bar{\sigma}_{T+} & \text{for } E_T \varepsilon_T \geq \bar{\sigma}_{T+} \end{cases}$$

$$\tau_{LT} = \begin{cases} G \gamma_{LT} & \text{for } -\bar{\tau}_{LT} \leq G \gamma_{LT} \leq \bar{\tau}_{LT} \\ -\bar{\tau}_{LT} & \text{for } G \gamma_{LT} \leq -\bar{\tau}_{LT} \\ \bar{\tau}_{LT} & \text{for } G \gamma_{LT} \geq \bar{\tau}_{LT} \end{cases}$$

that is assuming an elastic model for the longitudinal normal stress, and elastic-plastic models for transverse and shear stresses.

With such a lamina model, for a given twisting moment to axial load ratio, and for a given specimen type, elastic-plastic stress analysis can be very easilu performed assuming uniform strains, with incrementally increasing average stresses, Failure is assumed to occur when, in at least one lamina, the longitudinal normal stress becomes lower than the compressive failure limit (fiber buckling) or higher than the tensile failure limit (fiber breaking), or when equilibrium cannot be obtained (plastic instability).

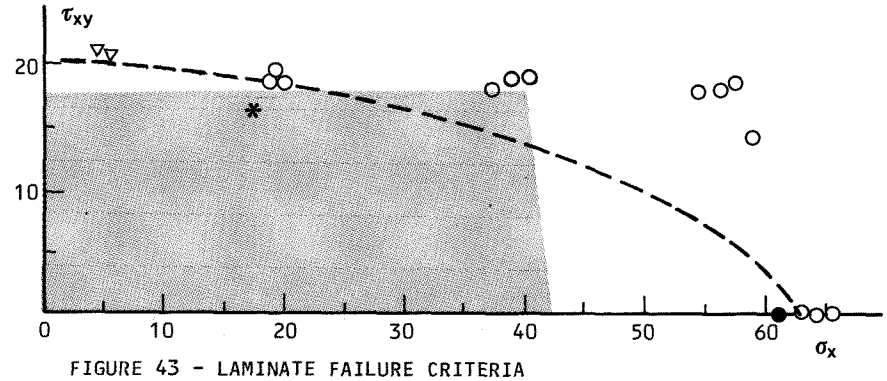

FIGURE 43 - LAMINATE FAILURE CRITERIA ORTHOTRPIC LAMINATE, "a"

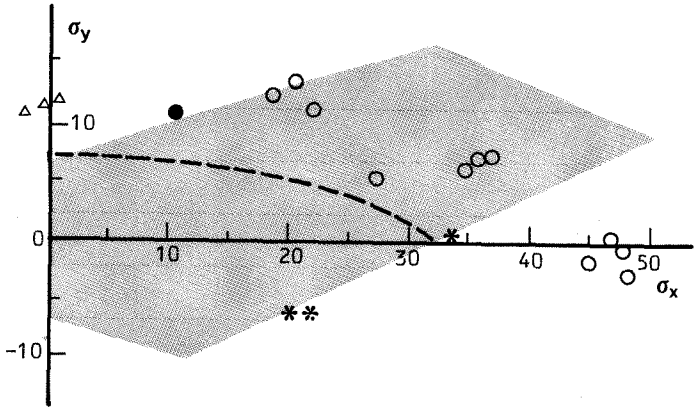

FIGURE 45 - LAMINATE FAILURE CRITERIA ORTHOTROPIC LAMINATE, "c"

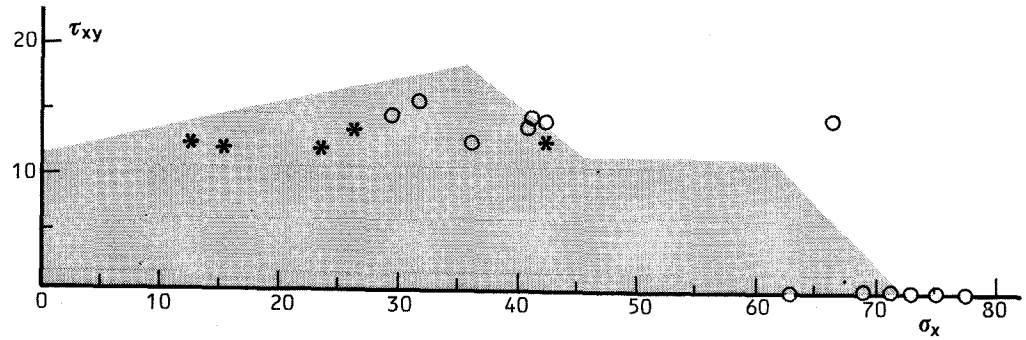

FIGURE 46 - LAMINATE FAILURE CRITERIA ANISOTROPIC LAMINATE, "a"

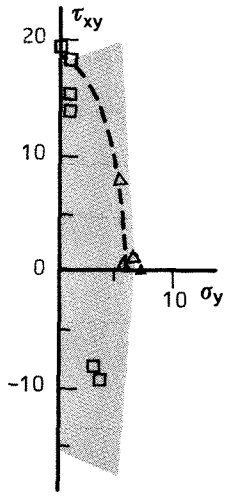

FIGURE 44 - LAMINATE FAILURE CRITERIA ORTHOTROPIC LAMINATE, "b"

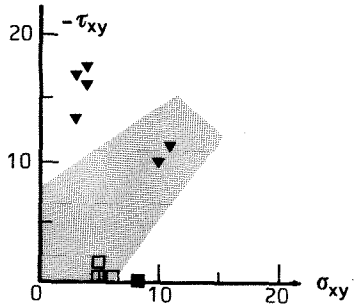

FIGURE 47 - LAMINATE FAILURE CRITERIA ANISOTROPIC LAMINATE, "b"

With this model failure envelopes can be mapped by means of a simple computer program. Such envelopes were actually computed and reported in figures 43-49 as dashed areas; the following parameters have been used for the computations:

$\bar{\sigma}_{L-} = -35\ kgmm^{-2}$; $\bar{\sigma}_{L+} = 160\ kgmm^{-2}$; $E_L = 4500\ kgmm^{-2}$

$\bar{\sigma}_{T-} = -3\ kgmm^{-2}$; $\bar{\sigma}_{T+} = 2\ kgmm^{-2}$; $E_T = 1000\ kgmm^{-2}$

$\bar{\tau}_{LT} = 1.5\ kgmm^{-2}$; $G = 500\ kgmm^{-2}$

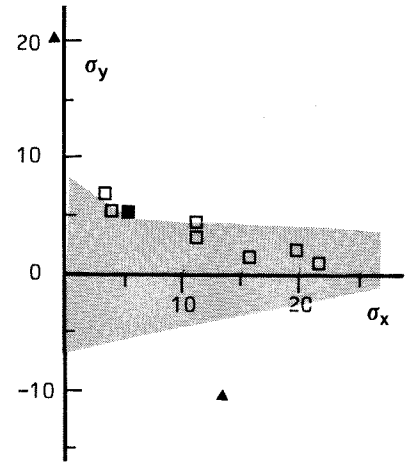

FIGURE 48 - LAMINATE FAILURE CRITERIA ANISOTROPIC LAMINATE, "c"

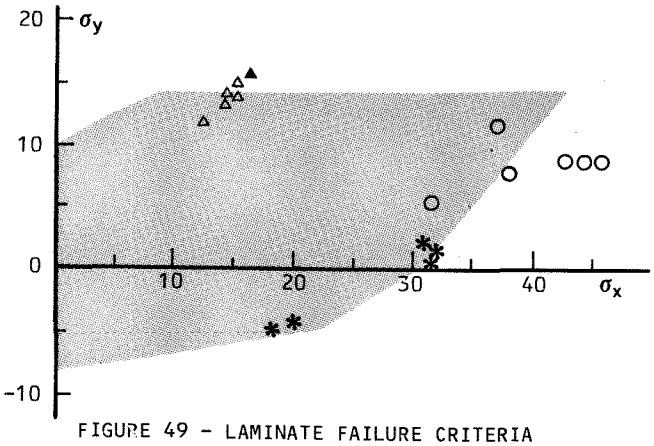

FIGURE 49 - LAMINATE FAILURE CRITERIA ANISOTROPIC LAMINATE, "d"

It appears clearly that the above proposed criterion, even if not completely satisfactory, have a remarkable agreement with experimental trends.

Obviously such a model could be easily refined taking into account some stress interaction within each lamina, and assuming fiber buckling stresses depending on the position in the stack.

Even so refined it will maintain its basic advantages, i.e.:

- only lamina parameters are required;
- interaction between laminae is taken into account, as the stresses in each lamina is dependent on the elastic-plastic deflection of the whole laminate;
- informations can be obtained on the relevant failure mode;
- the computation requires only a very simple program, that could be run also on a microcomputer.

Concluding Remarks

The result of the experimental work so far completed allow to draw the following preliminary conclusions:

- linear material model can be very accurate also for combined stress conditions;
- failure data from flat specimens don't show any definite influence from specimen width, at least above the minimum width tested (25.4 mm), and correlate quite well with tubular specimens data;
- interlaminar edge stresses in flat specimens and interlaminar traction forces (due to curvature) in tubular specimens do not seem to affect significantly failure;
- a practical failure criterion can be devised requiring only lamina parameters, which is based on elastic-plastic analysis, in uniform strain situations.

The future activity will include the completion of the experimental work, the study of non linear material behaviour, and the development and extensive checking of the proposed failure criterion.

References

1. V. Giavotto, V. Caramaschi, G.C. Maffioli, R&D on Composite Rotor Blades at Agusta, Seventh European Rotorcraft and Powered Lift Aircraft Forum, paper n. 62, Garmish-Partenkirchen (1981)

2. C.E. Covington, P.S. Baumgardner, Design and Production of Fiberglass Rotor Blades, in Fibrous Composites,in Structural Design (eds. E.M. Lenoe, D.W. Oplinger, J.J. Burke), Plenum Press (1980)

3. E.F. Olster, H.K. Reddick Jr., Preliminary Design of an Advanced Composite Rotor Hub for the HU-60A Black Hawk, in Fibrous Composites,in Structural Design (eds. E.M. Lenoe, D.W. Oplinger, J.J. Burke), Plenum Press (1980)

4. V. Giavotto, M. Borri, L. Puccinelli, F. Mussi, V. Caramaschi, Evaluation of Section Properties for Hollow Composite Beams, Fifth European Rotorcraft and Powered Lift Aircraft Forum, paper n. 35, Amsterdam (1979)

5. N.J. Pagano, The Role of Effective Moduli in the Elastic Analysis of Composite Laminates, in Composite Materials, Vol. 2 (vol. ed. G.P. Senedeckyj) Academic Press (1974)

6. S.W. Tsai, E.M. Wu, A General Theory of Strength for Anisotropic Materials, Journal of Composite Materials, vol. 5 (1971)

7. E.M. Wu, Phenomenological Anisotropic Failure Criterion, in Composite Materials, Vol. 2 (vol. ed. G.P. Senedeckyj), Academic Press (1974)

8. E.M. Wu, Failure Criteria to Fracture Mode Analysis of Composite Laminates, AGARD-CP-163, (1974)

9. A.H. Puppo, H.A. Evensen, Strength of Anisotropic Materials under Combined Stresses, AAIA Journal, Vol. 10, n. 4 (1972)

10. U. Hütter, H. Schelling, H. Kraus, An Experimental Study to Determine Failure Envelope of Composite Materials with Tubular Specimens under Combined Loads and Comparison between several Classical Criteria, AGARD-CP-163 (1974)

11. T.R. Guess, Biaxial Testing of Composite Cylinders: Experimental-Theoretical Comparison, Composites, Vol. 11, n. 7 (1980)

12. M.J. Owen, D.J. Rice, Biaxial Strength Behaviour of Glass Fiber Reinforced Polyester Resins, Composites, Vol. 12, n. 1, (1981)

13. D.M. Purdy, Composite Structures, International Symposium on Structural Mechanics Software, College Park, Maryland (1974)

14. V. Giavotto, M. Borri, P. Mantegazza, G. Ghiringhelli, V. Caramaschi, G.C. Maffioli, Anisotropic Beam Theory and Applications, to be presented at the Symposium on Advances and Trends in Structural and Solid Mechanics, Washington D.C. (october 1982)

15. R.M. Christensen, Mechanics of Composite Materials, John Wiley & Sons (1979).